

## SIMP: Single Microwave Photon detection

D. Alesini, D. Babusci, M. Beretta, B. Buonomo, F. Chiarello (CNR-IFN), L. Foggetta, G. Felici, A. Gallo, D. Di Gioacchino, C. Gatti (Resp. Naz.), C. Ligi (Resp. Loc.), G. Maccarrone, F. Mattioli (CNR-IFN), G. Papalino(Tecn.), G. Pileggi (Tecn.), A. Rettaroli (Dott.), F. Tabacchioni (Tecn. INAF), G. Torrioli (CNR-IFN), S. Tocci (Bors.), A. Tudorache (student)

### 1 Introduction

SIMP has the ambition of developing superconducting devices sensitive to single photons in the frequency range between 10 and 100 GHz. The collaboration, coordinated by LNF, is engaged in two main activities: design, fabrication and test of a Transition Edge Sensor (INFN-Pi, TIFPA, CNR-NEST, INRIM); design, fabrication and test of a Current Biased Josephson Junction (LNF, INFN-Salerno, CNR-IFN). In this report, we focus on the second activity in which the LNF group has been more engaged. The activity is carried out at the COLD (CryOgenic Laboratory for Detectors) laboratory at LNF.

Superconducting circuits based on Josephson junctions <sup>1)</sup> (JJ) are fabricated by standard lithographic technologies and can be integrated in complex systems, with an extremely high flexibility and controllability. The nonlinearity of the JJ allows the realization of systems behaving as artificial atoms, with typical level spacing of the order of few GHz up to tens of GHz. All these characteristics make them interesting as detectors for microwave single photons. In this report we briefly describe the first DC characterization of Al JJs in a dilution refrigerator at temperatures down to 40 mK.

### 2 Josephson Junction fabrication parameters

Al JJs were fabricated in Rome at CNR-IFN. Electron Beam Lithography (EBL) technique was used to obtain the submicrometric junctions needed for the fabrication of the Josephson elements. The devices were realized in aluminum with a direct writing approach followed by a shadow mask evaporation process <sup>2)</sup> described in Fig. 1. The aluminum is deposited with thin film deposition techniques and it is then thermally oxidized achieving an Al<sub>2</sub>O<sub>3</sub> layer by exposing the metal surface to a controlled oxygen pressure for a time of the order of few minutes.

The product “Pressure × Time” finely controls the tunnel resistance. A second evaporation of aluminum, tilted with respect the first one, uses the shadows formed by two different deposited polymers to realize junctions and complex structures. The chip design is shown in Fig. 2. A 5 minutes oxidation period at a pressure of 5 mbar was used with an estimated values for the specific critical-current density and specific capacitance of:

$$\begin{aligned} J_c &= 30 \text{ nA}/\mu\text{m}^2 \\ c_j &= 50 \text{ fF}/\mu\text{m}^2 \end{aligned}$$

In Tab. 1 we report the estimated characteristic-values of the two larger junctions (in the following number 5 and 6).

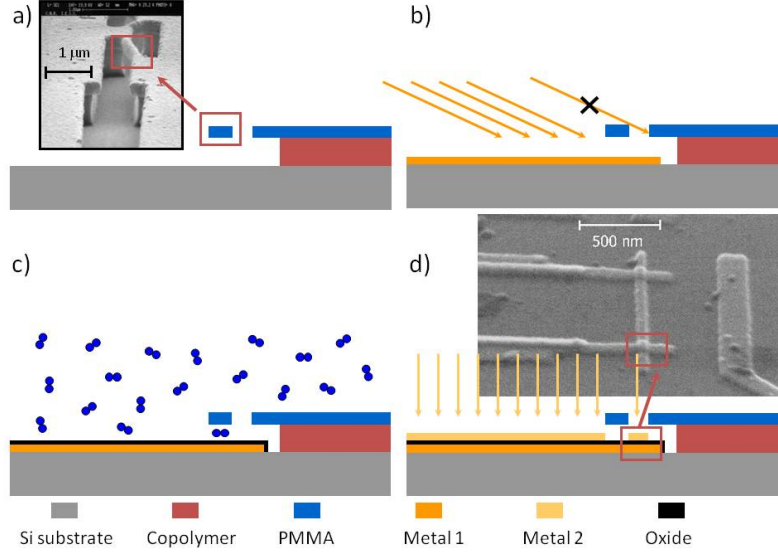


Figure 1: Block scheme of the shadow evaporation technique: a) two electronic resist (copolymer and PMMA) EBL and development. Inset: SEM image. b) First metal evaporation. c) Oxidation of the metal surface to obtain the tunneling barrier. d) Second metal evaporation.

Table 1: Expected junctions parameters

JJ N.	Area ( $\mu\text{m}^2$ )	$I_c(\mu\text{A})$	C(pF)	$E_c = 2e^2/C$	$E_j = \Phi_0 I_c / 2\pi$	$f_p = \sqrt{2E_c E_j} / 2\pi$
5	4	0.12	0.2	$1.6 \mu\text{eV}$	0.24 meV	6.7 GHz
6	8	0.23	0.4	$0.8 \mu\text{eV}$	0.48 meV	6.7 GHz

### 3 Experimental setup

The chip was mounted inside the mixing chamber bath of a plastic dilution refrigerator, property of CNR-IFN (Fig. 3), a Leiden Cryogenics MCK50-100, refurbished and put in operation at LNF. A temperature of 43 mK was reached after few attempts. With about 100 liters of LHe we could keep the system cold and perform measurements for 3 days.

JJs are bonded to the chip and connected through twisted pairs of phosphor-bronze wires to Fischer connector at the 300 K top-part of the refrigerator. Each JJ has four contacts, two in common, to allow readout using the four-wires-measurement technique. No filtering was used at the cold stage. At room temperature, we measured about  $25 \Omega$  impedance of the twisted wires. Twisted pairs are connected to coaxial cables and external instruments through low-pass filters with 600 kHz bandwidth. A sketch of the experimental setup is shown in Fig. 4. The JJs are biased with a triangular voltage-signal generated with a wavefunction generator (Keysight Technologies 33521B 30 MHz) at the frequency of 314 Hz applied to a  $200 \text{ k}\Omega$  resistor. The voltage across the resistor is measured through a preamplifier (EGG 5113) whose output is acquired by an ADC board (NI USB-6366, X Series). EGG 5113 has a bandwidth of 1 MHz and noise of  $4 \text{ nV}/\sqrt{\text{Hz}}$ . The bias current is estimated by dividing the measured voltage by the resistance value. A second

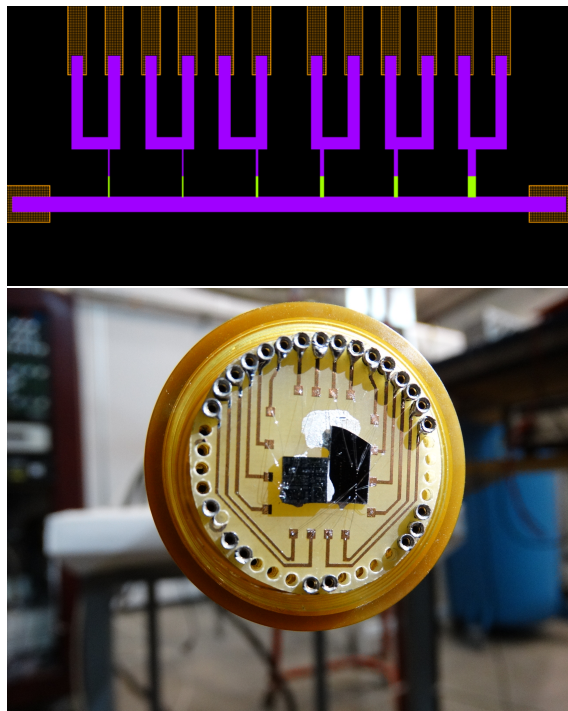


Figure 2: Top: Design of the chip with 6 Al JJs (yellow) and wiring (purple). The junctions are  $2\ \mu\text{m}$  long and  $500\ \text{nm}$ ,  $500\ \text{nm}$ ,  $1\ \mu\text{m}$ ,  $1.5\ \mu\text{m}$ ,  $2\ \mu\text{m}$  and  $4\ \mu\text{m}$  long. Bottom: Chip mounted on the mixing chamber of the dilution refrigerator. Beside the chip with JJs a second chip with Nb DC-Squid is visible.

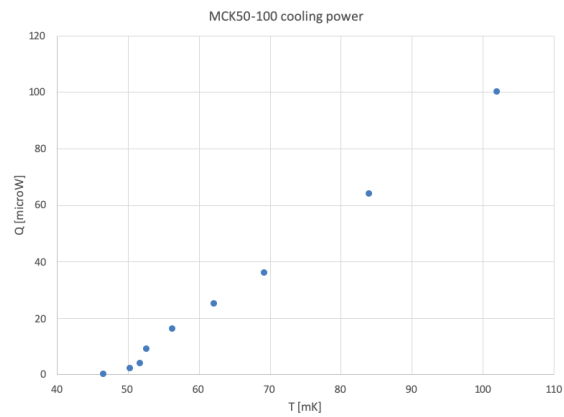


Figure 3: Top: Dilution refrigerator of CNR-IFN, a Leiden Cryogenics MCK50-100, in the COLD laboratory at LNF. Bottom: Cooling power vs temperature measured at LNF.

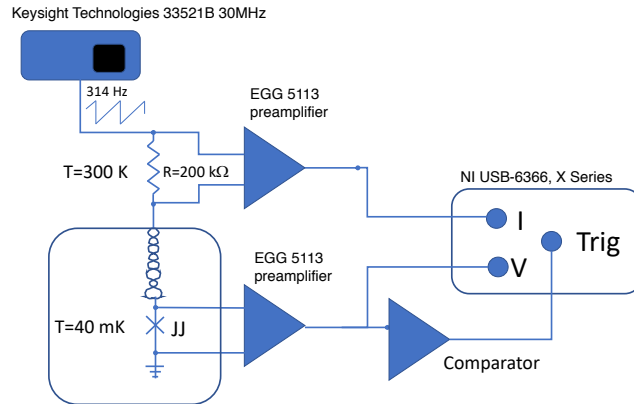


Figure 4: Sketch of the experimental setup.

preamplifier reads the voltage across the JJ under test. The output of the amplifier is both acquired with the ADC board and sent to a comparator that generates a trigger signal to synchronize the acquisition with the transition of the junction from the superconducting to the resistive state.

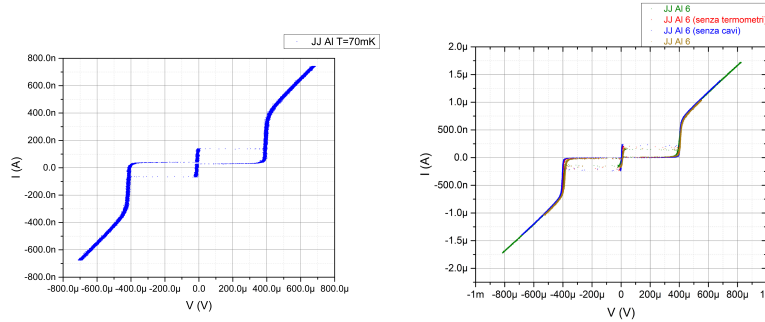


Figure 5: I-V measured for junction N.5 (left) and 6 (right).

#### 4 Josephson Junction I-V measurement

In Fig. 5 we show the measured I-V relations for the JJs number 5 (left panel) and number 6 (right panel) at  $T=70$  mK. We observe escape currents of 120 nA and 250 nA, consistent with the values in Tab. 1. For junction n.6 we show different curves measured by unplugging the cryostat diagnostic devices (thermometers and vacuum gauges). We observe an increase in the value of the escape current, from about 200 to 250 nA, signaling a consistent amount of noise induced into the junction by the present setup. For both junctions we observe gap voltage  $V_{gap} = 400 \mu\text{V}$ , a bit smaller than expected from twice the superconducting gap of Al  $\Delta_{Al} = 340 \mu\text{eV}$ . The resistance of the normal branch is measured as  $1000 \Omega$  and  $500 \Omega$  for junctions number 5 and 6, respectively. From the measured  $V_{gap}$  and  $R_N$  and BCS<sup>3)</sup> relations we can estimate the critical temperature and critical current as:

$$I_c = \frac{V_{gap} \pi}{R_N 4}$$

$$T_c = \frac{V_{gap}}{3.53 k_B}$$

leading to  $T_c = 1.3$  K and  $I_c = 0.32$  and  $0.63 \mu\text{A}$  for junction number 5 and 6, respectively. The values of the critical current are a bit higher but of the same order of magnitude of the observed ones.

#### 5 Measurement of the JJ Escape Currents

A deep understanding of the dynamics, dissipation and noise in JJs is obtained from the study of the distribution of the escape currents at different temperatures<sup>4, 5, 6, 7, 8, 9, 10, 11, 12, 13)</sup>. We show the measured distributions in Fig. 6 and 7. A distinctive feature of these measurements is the decreasing of the mean and rms of the distributions with increasing temperature. While the reduction of the mean is expected with increasing temperature, the behaviour of the rms strongly depends of loss mechanism in the junction. In particular, in our experimental setup no filtering was used at the cold stage so that the leads show a characteristic impedance on the order of the free space impedance  $Z_0 = 377 \Omega$ . This generates a damping of high frequency oscillation of the junction that inhibits the thermal activation and consecutive escape to the resistive state of the junction itself. Since the damping effect increases with temperature, the escape rate, and therefore the rms of the distribution, decreases with increasing temperature. A detailed study is ongoing to interpret these data through the comparison with theoretical models and numerical simulations.

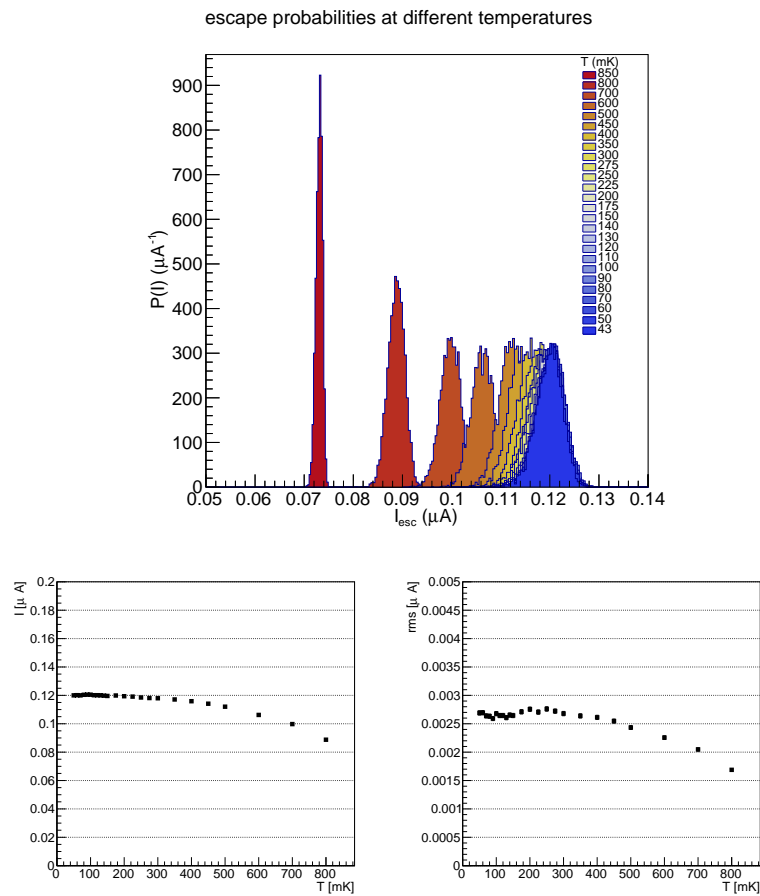


Figure 6: Top: Escape current distribution for junction number 5 as a function of temperature. Bottom: Mean and rms of the distributions.

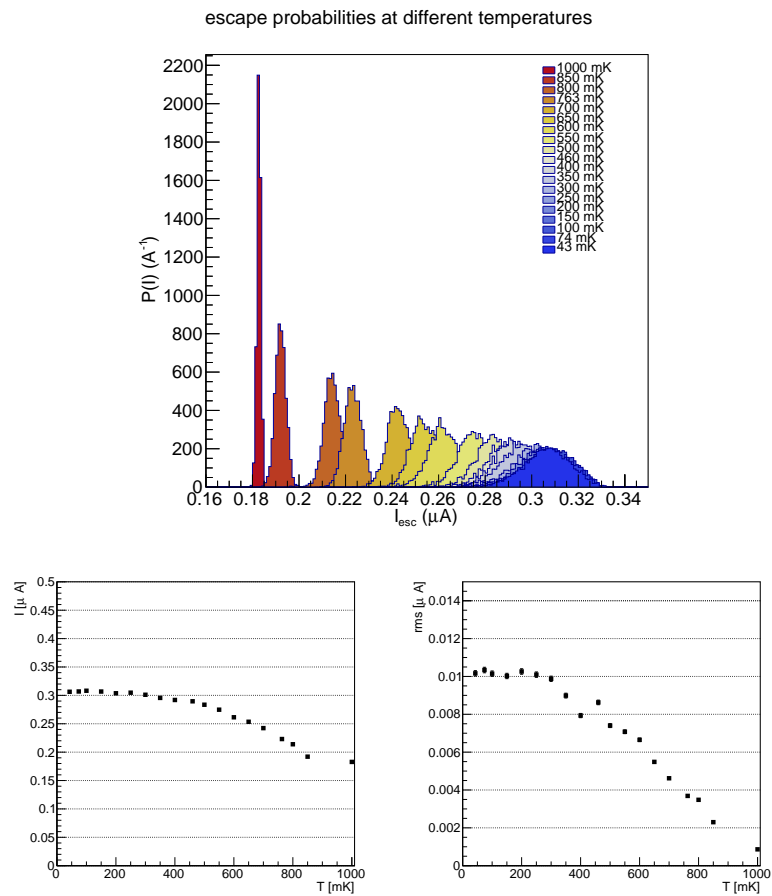


Figure 7: Top: Escape current distribution for junction number 6 as a function of temperature. Bottom: Mean and rms of the distributions.

## References

1. A. Barone and G. Paternò, "Physics and Application of the Josephson Effect", John Wiley & Sons, Inc. (1982).
2. B. Buonomo et al., "Aluminium single-electron transistors studied at 0.3 K in different transport regimes," J. Appl. Phys. 89, 6545 (2001).
3. M. Tinkham "Introduction to Superconductivity" McGraw-Hill, Inc. (1996).
4. D.Massarotti et al. Low Temperature Physics/Fizika Nizkikh Temperatur, 2012, v. 38, No. 4, pp. 336347.
5. M-H Bae et al. PHYSICAL REVIEW B 79, 104509 (2009).
6. L. Longobardi et al., PRL 109, 050601 (2012).
7. G. Castellano et al. Journal of Applied Physics 86, 6405 (1999)
8. J M Kivioja et al 2005 New J. Phys. 7 179
9. H.F. Yu et al., PRL 107, 067004 (2011).
10. J.C. Fenton and P.A. Warburton arXiv:0807.4502v1
11. Kivioja PRL 94, 247002 (2005)
12. Yoon arXiv:1012.0541
13. E.B. Jacob et al. Phys.Rev. A 26 (1982).